Talanta 88 (2012) 765–768

Contents lists available at SciVerse ScienceDirect

Talanta

journal homepage: www.elsevier.com/locate/talanta

Short communication

Protein functionalized titania particle as a nanocarrier in a multiple signal antibody amplification strategy for ultrasensitive chemiluminescent immunoassay

Zhenxing Wang, Jing Han, Hongfei Gao, Cuifang Li, Zhifeng Fu*

Key Laboratory of Luminescence and Real-Time Analysis (Ministry of Education), College of Pharmaceutical Sciences, Southwest University, Chongqing 400716, China

ARTICLE INFO

Article history:
Received 20 September 2011
Received in revised form
21 November 2011
Accepted 1 December 2011
Available online 8 December 2011

Keywords:
Titania nanoparticle
Chemiluminescent immunoassay
Nanocarrier
Signal amplification
Human IgG

ABSTRACT

A simple and sensitive method for amplified chemiluminescent immunoassay has been developed by using multiple signal antibodies functionalized titania nanoparticle as tracer. This nanocomposite was fabricated by sequentially conjugating bovine serum albumin and horseradish peroxidase-labeled antibody onto the surface of titania nanoparticles using glutaraldehyde as the linkage. After a sandwich immuno-binding process, the captured nanocomposite tracer greatly catalyzed the luminol chemiluminescence reaction to produce a strong signal. Human IgG was detected as a model analyte, and a linear range of 0.5–200 ng mL^{-1} was obtained. The detection limit of the proposed method was 0.1 ng mL^{-1}, which was 50-folds lower than that using the traditional tracer. The reproducibility, the stability and the specificity of the proposed immunoassay method were acceptable. The results for real sample analysis also demonstrated its application potential in some important areas such as clinical diagnosis.

1. Introduction

Extensive research interests and great efforts have been long focused on improving sensitivity of disease-related biomarkers detection for its promising potential in clinical disease screening and early diagnostic application [1–4]. In recent years, unique physical and chemical properties of nanoparticles (NPs) offer excellent prospects for designing highly sensitive immunoassay methods due to the enormous signal enhancement associated with using NPs as tracers [5–13,15–20].

Two strategies using NPs as tracers can be adopted to develop highly sensitive immunoassay method. One is the utilization of the special electrical, optical, catalytic and magnetic properties of nano-sized materials for signal transduction [5–9]. For example, the high fluorescence intensity of quantum dots [5,6], and the enhanced surface plasmon resonance of gold NPs [7,8] have resulted in improved sensitivity of fluorescent and surface enhancement Raman spectroscopic immunoassay. The second one for the improved sensitivity attributes to numerous signal molecules contained in a single nano-sized tracer [10–13]. The single nano-sized tracer containing large numbers of signal molecules thus produces a much higher signal than the single tracer containing only one or several signal molecules (traditional tracer). For instance, the gold NPs used as tracer can be chemically [10,11] or electrochemically [12] dissolved to form numerous Au^{3+}, and the resulting Au^{3+} can be detected by chemiluminescence (CL) or electrochemical signal, respectively, which shows greatly improved sensitivity. However, the dissolving process need to be conducted under extremely harsh conditions, such as strong oxidant and strong acid, thus should be further improved [14]. Another successful example is europium oxide NPs for phosphorescent immunoassay, which shows much stronger phosphorescence than single europium compound used as tracer [13]. It is noticed that the preparation of nano-sized tracer is sometimes challenging and difficult. Up to now, only several of the usual tracers have already been prepared in a nano size and used for conjugating biomolecules.

To overcome the difficulty in the preparation of nano-sized tracer, an alternative approach for the same purpose is proposed, which use currently existing NPs as nanocarriers to load large amounts of signal molecules [15–20]. These easily prepared NPs with good biocompatibility, such as silica NP [15–18], gold NP [19], polystyrene NP [20], can be facilely functionalized through internal doping or surface modification. For example, with the reverse microemulsion protocol, $Ru(bpy)_3Cl_2$ [15,16], luminol [17] or horseradish peroxidase (HRP) [18] were doped into silica NPs to act as CL or electrochemical immunoassay tracer. However, the internal doping signal small molecules in NPs suffer the challenge of leakage [21]. Electrostatic adsorption and covalent binding are also frequently applied to prepare NPs functionalized with signal

* Corresponding author. Tel.: +86 23 6825 0184; fax: +86 23 6825 1048.
E-mail address: fuzf@swu.edu.cn (Z. Fu).

0039-9140/$ – see front matter © 2011 Elsevier B.V. All rights reserved.
doi:10.1016/j.talanta.2011.12.003

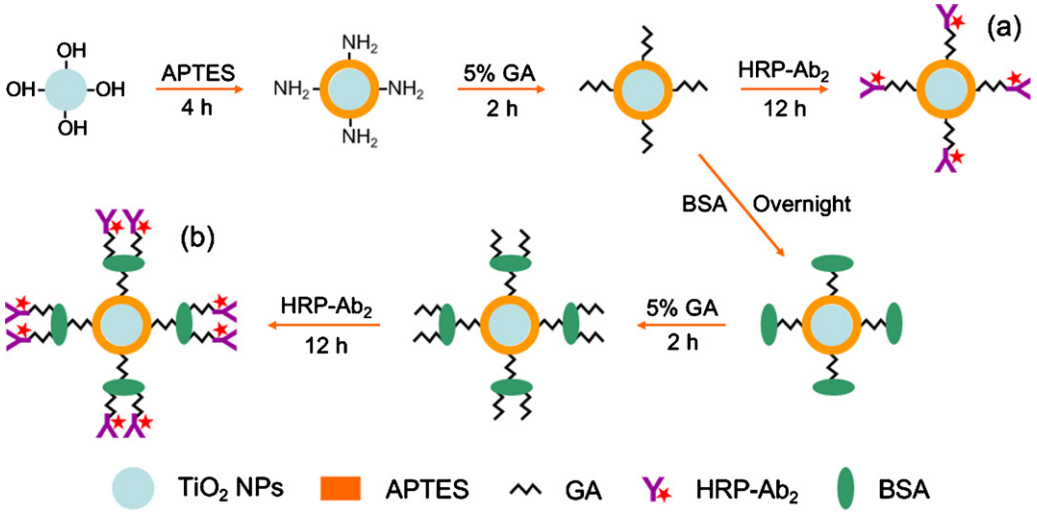

Fig. 1. The schematic illustration of the preparation of (a) TiO_2/HRP-Ab_2 and (b) TiO_2/BSA/HRP-Ab_2.

molecules. With this strategy, many nano-sized carriers were used to load HRP [1,22], poly(guanine) [23], and luminol [24], etc. It should be mentioned that these tiny NPs with small surface area are unfavorable for protein-binding. Furthermore, the biological tags are directly conjugated to the NPs, which could affect the activity and stability of the bound biomolecules due to the potential toxicity of NPs.

Titania NPs (TiO_2 NPs) are a promising nano-sized carrier for enzyme probe loading since this NP provides hydroxy group-functionalized surface for covalent conjugation of protein. Also, the activity and the stability of biomolecule can be well maintained on this biocompatible NP. Here, we proposed a novel enhanced CL immunoassay (CLIA) by using bovine serum albumin (BSA) functionalized TiO_2 NPs to load HRP-labeled signal antibody. This nano-sized tracer increased the amount and retained the activity of the bound HRP-labeled antibody, and thus showed lower detection limit than the traditional HRP-labeled antibody and TiO_2 NPs conjugated HRP-labeled antibody.

2. Materials and methods

2.1. Reagents and materials

Human IgG (HIgG), mouse monoclonal antibody for HIgG (Ab_1) and HRP labeled goat polyclonal antibody for HIgG (HRP-Ab_2) were all purchased from Beijing Biosynthesis Biotechnology Co., Ltd. BSA were provided by Beijing Dingguo Biotechnology Co., Ltd. TiO_2 NP suspension (5%, product number: 643114) with a diameter of 50 nm was obtained from Sigma–Aldrich Chemical Co., Ltd. Triethoxy-3-aminopropylsilane (APTES, 99%) was provided by Aladdin Chemistry Co., Ltd. Glutaraldehyde (GA) was provided by Chengdu Kelong Chemical Reagent Co., Ltd. SuperBlock® T20 (Thermo Fisher Scientific Inc.) was used as blocking buffer to block the residual reactive sites on the microplate. The serum and urine samples were provided by three healthy adult volunteers. All solutions used throughout this study were prepared with ultra-pure water (18.2 MΩ) supplied by an ELGA PURELAB classic system. All other chemicals were analytical grade and used without further purification.

2.2. Apparatus

The polystyrene 96-well high-affinity microplate was provided by Greiner Bio-One Biochemical Co., Ltd. The CL measurements were carried out on a MPI-A CL analyzer (Xi'an Remax Electronic Science & Technology Co., Ltd.) equipped with a photomultiplier operated at −800 V. The morphologies of TiO_2 NPs and nano-sized tracer were characterized using a transmission electron microscope (TEM, F-7500, Hitachi Instrument Co., Ltd.).

2.3. Preparation of TiO_2/BSA/HRP-Ab_2 nanocomposite

As illustrated in Fig. 1, the highly luminous nano-sized tracer was prepared by sequentially binding BSA and HRP-Ab_2 onto the surface of TiO_2 NPs using a classic GA-linkage method. Firstly, 100 μL of TiO_2 NP suspension was silanized for 4 h using 1.5 mL of APTES solution (APTES–methanol–H_2O, 1:94:5, v/v/v) containing 1 mM acetic acid to obtain amino group-functionalized NPs. The resulted TiO_2 NPs were then washed three times with water, and dispersed in 0.10 M phosphate buffer at pH 7.0 (PBS) containing 5% GA for about 2 h with shaking. After thorough washing, the NPs were re-dispersed in PBS. Ten milligram of BSA were added into the activated NPs and stood for 12 h at 4 °C with shaking, to obtain BSA-loaded TiO_2 NPs. Afterwards, the BSA-loaded TiO_2 NPs (TiO_2/BSA) were dispersed in PBS containing 5% GA for another 2 h. Finally, the GA-linked TiO_2/BSA NPs were incubated with HRP-Ab_2 in PBS for 12 h at 4 °C with shaking, to prepare TiO_2/BSA/HRP-Ab_2 nanocomposite tracer. The product was washed with PBS five times to remove excess HRP-Ab_2, and kept at 4 °C in PBS unless use.

2.4. Sandwich CLIA procedure

The TiO_2/BSA/HRP-Ab_2 nanocomposite was used as the tracer for an enhanced CLIA. HIgG was chosen as a model analyte in this study, and a classic sandwich immunoassay procedure was adopted. In a typical experiment, a polystyrene 96-well microplate was coated with 100 μL of Ab_1 (10 μg mL^{-1} in 0.10 M Tris–HCl buffer, pH 8.0) per well overnight at 4 °C. After removal of the unbound Ab_1, each well was washed three times with 300 μL of washing buffer (PBS containing 0.05% Tween 20). After that, the plate was blocked with 200 μL of blocking buffer per well for 1.5 h at 37 °C, and washed three times with the washing buffer. One hundred microliter of sample solution were pipetted into the well and incubated at 37 °C for 1.5 h. After three times washing, 100 μL of TiO_2/BSA/HRP-Ab_2 nanocomposite tracer (TiO_2 concentration 50 μg mL^{-1}) was added into the well and incubated for 1.5 h at 37 °C. Following the thorough washing, 100 μL of CL reagent composed of luminol and p-iodophenol (PIP) were injected into each

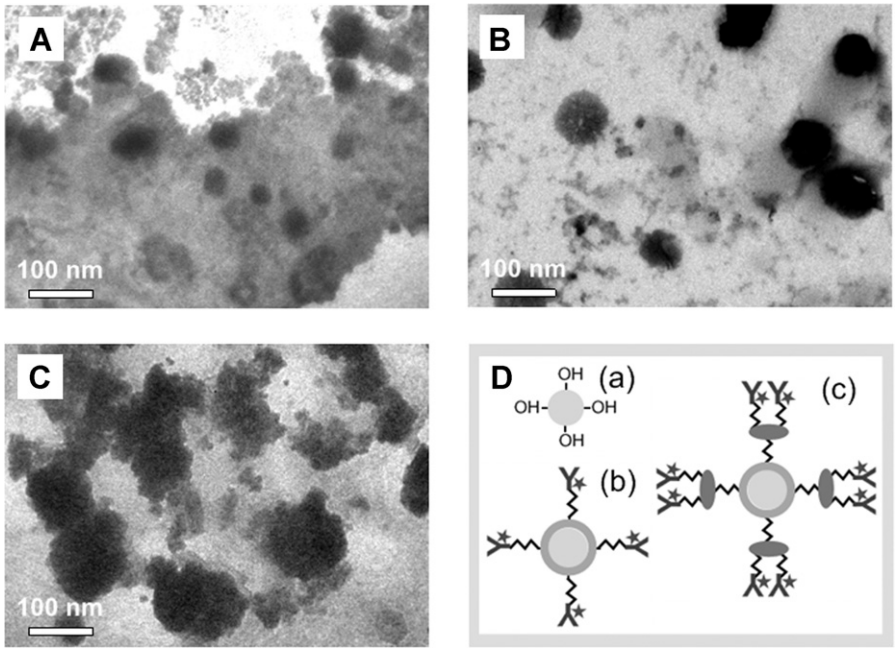

Fig. 2. The TEM images of TiO_2 NPs (A), TiO_2/BSA (B) and TiO_2/BSA/HRP-Ab_2 (C). The schematic diagrams of the three NPs are shown in D.

well. Finally, the CL peak emission was recorded with a photomultiplier after injection of H_2O_2. All the CL signals were calibrated by subtracting the blank response.

3. Results and discussion

3.1. Characterization and signal amplification of TiO_2/BSA/HRP-Ab_2 nanocomposite

In the present work, TiO_2 NP was employed as the carrier for HRP-Ab_2. TEM was used to characterize the preparation of TiO_2/BSA/HRP-Ab_2 nanocomposite. It can be seen that the spherical bare TiO_2 NPs showed a mean diameter of 50 nm (Fig. 2A). After the NPs were coupled with BSA, the mean diameter increased to about 70 nm (Fig. 2B). And that, TiO_2/BSA nanocomposite was coupled with HRP-Ab_2 to form TiO_2/BSA/HRP-Ab_2 nano-sized tracer with a diameter about 100 nm (Fig. 2C). The successive increase of NP size demonstrated that BSA and HRP-Ab_2 were sequentially coupled with TiO_2 NP.

In this study, signal amplification of the TiO_2/BSA/HRP-Ab_2 nanocomposite was confirmed in a typical sandwich CLIA. For 1.0 ng mL^{-1} HIgG, almost no signal and only very weak signal were observed when HRP-Ab_2 and TiO_2/HRP-Ab_2 were adopted, respectively. When TiO_2/BSA/HRP-Ab_2 at the same concentration was used instead of HRP-Ab_2 and TiO_2/HRP-Ab_2, strong CL signal was collected. The above results not only strongly demonstrated that HRP-Ab_2 was successfully coupled to the TiO_2 NPs through the "bridging" effect of BSA and still maintained its good activity, but also confirmed the validity of the signal amplification of TiO_2/BSA/HRP-Ab_2 as tracer. This amplification effect can be attributed to three reasons. Firstly, after the amino group-rich BSA molecules were bound to TiO_2 NPs, TiO_2/BSA nanocomposite possessed more chemical linking sites and larger loading surfaces than amino group-functionalized bare TiO_2 NPs. Thus TiO_2/BSA/HRP-Ab_2 nano-sized tracer carried more signal molecules than the conventional tracers. Secondly, with the BSA-mediated conjugation strategy, the steric hindrance between the NP and the antigen was greatly decreased. Therefore, the immuno-binding between the TiO_2/BSA/HRP-Ab_2 signal antibody and the antigen could occur more easily. Thirdly, the mediated BSA molecules provided a more biocompatible microenvironment for the signal antibody. Due to the potential toxicity of NPs, the activity and stability of a signal biological molecule directly connected to a NP may be damaged [25]. Here, BSA molecule was used as a "bridge" to connect the signal antibody and the NP, thus provided an ideal biocompatibility for the HRP-Ab_2 signal antibody. The TiO_2/BSA/HRP-Ab_2 nanocomposite stored in PBS at 4 °C showed no obvious activity change after two months storing. While the HRP labeled antibodies were directly bound to the bare TiO_2 NPs, a mass of particle aggregation and obvious activity loss were observed for this TiO_2/HRP-Ab_2 nanocomposite after only one month of storage.

The reproducibility on the preparation of TiO_2/BSA/HRP-Ab_2 NPs was investigated by performing sandwich immunoassay with 5 batches of nanocomposites. The relative standard deviation (RSD) of the CL responses for a sample at 50 ng mL^{-1} was 8.7%. This result showed an acceptable preparation reproducibility of this nanocomposite.

3.2. Optimization of CLIA conditions

The performance of immunoassay is usually affected by certain parameters such as the incubation time, the blocking time, and the concentration of the tracer. Fig. S-1 in the Supplementary Data showed the effect of the incubation time on the CL response from HIgG at 50 ng mL^{-1}. It was found that the CL response from the bound tag increased sharply with the incubation time and almost trended to the maximum at 90 min, indicating the immuno-binding reached the saturation. Blocking buffer was used to reduce the non-specific binding effect. The background signal resulting from the non-specific binding decreased with the increase of the blocking time in the range of 30–90 min. After 90 min, the CL signal resulting from the immuno-binding displayed a little decrease because the thick blocking layer increased the steric effect. Thus 90 min was chosen as the optimal blocking time. The effect of the dilution time of the TiO_2/BSA/HRP-Ab_2 nano-sized tracer on the CL response was investigated using HIgG at 50 ng mL^{-1} and PBS (as a blank) in parallel. When the dilution time of the nano-sized tracer was below 1:100 (TiO_2 concentration 50 μg mL^{-1}), the response

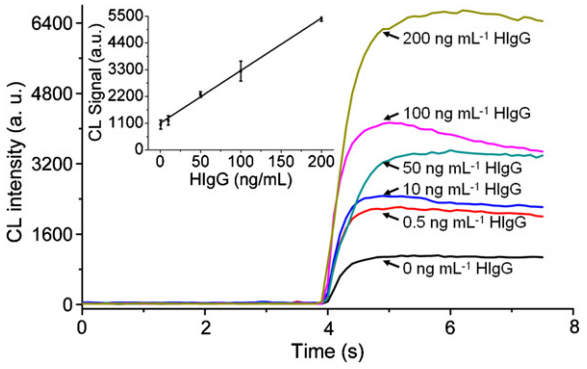

Fig. 3. The dose–response curve for CLIA using TiO_2/BSA/HRP-Ab_2 as tracer. Inset: calibration curve. All the tests were under the optimal conditions, and $n = 5$ for each point.

subtracting background decreased with the dilution time due to the non-specific binding (Fig. S-2). Therefore the dilution time of 1:100 was adopted since it provided the highest signal.

Some factors affecting the CL reaction were also investigated. Fig. S-3 in the Supplementary Data showed the effect of the CL substrate pH on the CL signal. The CL signal increased with the pH value in the range of 7.0–8.5, and began to decrease when the pH value was higher than 8.5. Therefore, 8.5 was chosen as the optimal pH value for the CL substrate. The effects of the concentrations of luminol, PIP and H_2O_2 were also studied in detail. The optimal concentrations for the three reagents were 0.05, 0.05 and 5 mM, respectively.

3.3. Analytical performance, specificity and real samples application

Under the optimal conditions, the performances of the three tracers were compared for the aforementioned sandwich immunoassay. The linear ranges were 0.5–200 ng mL^{-1}, 5–200 ng mL^{-1} and 20–300 ng mL^{-1} for TiO_2/BSA/HRP-Ab_2, TiO_2/HRP-Ab_2 and HRP-Ab_2, respectively. The correlation coefficients (R^2) for the three tracers were 0.9977, 0.9946 and 09943, respectively. The dose–response curve for CLIA using TiO_2/BSA/HRP-Ab_2 as tracer was shown in Fig. 3. The RSD of 5.4% for a sample at 50 ng mL^{-1} showed an acceptable detection reproducibility.

To investigate the potential interfering effects, we spiked some common cations and anions into HIgG at 50 ng mL^{-1}, and compared the resulted CL signals with that from a non-spiked HIgG standard sample at the same concentration. No obvious difference was observed between them when the concentrations of these cationic and anionic species were 100 times higher than those in normal human serums. The interfering effects of some biomolecules such as rabbit IgG and BSA were also investigated by spiking the two proteins at 50 ng mL^{-1} into the HIgG samples at the same concentration. As shown in Fig. S-4, a similar result was obtained, which demonstrated that this immunoassay method is not tended to be interfered by some potential interfering species in biological samples.

In order to estimate the application potential of this CLIA method using the nano-sized tracer, the levels of HIgG in three healthy human sera and two healthy human urines were evaluated with this method. Before the assay, the real samples were diluted appropriately to ensure that the HIgG concentrations were in the linear range. The HIgG levels were determined to be 8.9, 10.4 and 13.6 mg mL^{-1} in the three human sera, and 2.1 and 2.6 μg mL^{-1} in the two human urines, which were consistent with the clinical reference [26,27]. Known amounts of HIgG standards were spiked into the diluted samples to perform the recovery tests. From Table S-1 in the Supplementary Data, the recoveries for the spiked HIgG were between 92% and 108%, and the RSDs were all less than 7.4%, indicating the feasibility of proposed TiO_2/BSA/HRP-Ab_2 tracer.

4. Conclusion

In conclusion, we synthesized a novel TiO_2/BSA/HRP-Ab_2 nano-sized tracer for highly sensitive CLIA. Compared with the traditional tracers, it can greatly increase the surface coverage of HRP-Ab_2 molecules on NP, and avoid the damage on the activity and the stability of biomolecule, thus showing a wide linear range and a low detection limit. This strategy opens up a new possibility for analyzing very low levels of disease markers, biothreat agents, or environmental pollutions in complex biological matrixes that cannot be detected by those conventional methods.

Acknowledgments

This work was financially supported by the Natural Science Foundation of China (21175111, 20805036 and 21035005), and the Program for New Century Excellent Talents in University (NCET-10-0699).

Appendix A. Supplementary data

Supplementary data associated with this article can be found, in the online version, at doi:10.1016/j.talanta.2011.12.003.

References

[1] Y.F. Wu, C.L. Chen, S.Q. Liu, Anal. Chem. 81 (2009) 1600–1607.
[2] S.P. Song, Y. Qin, Y. He, Q. Huang, C.H. Fan, H.Y. Chen, Chem. Soc. Rev. 39 (2010) 4234–4243.
[3] G.S. Lai, F. Yan, J. Wu, C. Leng, H.X. Ju, Anal. Chem. 83 (2011) 2726–2732.
[4] A. Merkoçi, Biosens. Bioelectron. 26 (2010) 1164–1177.
[5] M.G. Warner, J.W. Grate, A. Tyler, R.M. Ozanich, K.D. Miller, J.L. Lou, J.D. Marks, C.J. Bruckner-Lea, Biosens. Bioelectron. 25 (2009) 179–184.
[6] W. Chen, C.F. Peng, Z.Y. Jin, R.R. Qiao, W.Y. Wang, S.F. Zhu, L.B. Wang, Q.H. Jin, C.L. Xu, Biosens. Bioelectron. 24 (2009) 2051–2056.
[7] J.S. Mitchell, T.E. Lowe, Biosens. Bioelectron. 24 (2009) 2177–2183.
[8] J. Yuan, R. Oliver, J. Li, J. Lee, M. Aguilar, Y. Wu, Biosens. Bioelectron. 23 (2007) 144–148.
[9] Z.P. Wang, J.Q. Hu, Y. Jin, X. Yao, J.H. Li, Clin. Chem. 52 (2006) 1958–1961.
[10] H.M. Zhang, W.T. Li, Z.H. Sheng, H.Y. Han, Q.G. He, Analyst 135 (2010) 1680–1685.
[11] A.P. Fan, C. Lau, J.Z. Lu, Anal. Chem. 77 (2005) 3238–3242.
[12] C. Leng, G.S. Lai, F. Yan, H.X. Ju, Anal. Chim. Acta 666 (2010) 97–101.
[13] J. Feng, G.M. Shan, A. Maquieira, M.E. Koivunen, B. Guo, B.D. Hammock, I.M. Kennedy, Anal. Chem. 75 (2003) 5282–5286.
[14] C.F. Duan, Y.Q. Yu, H. Cui, Analyst 133 (2008) 1250–1255.
[15] L.H. Zhang, S.J. Dong, Anal. Chem. 78 (2006) 5119–5123.
[16] X. Hun, Z.J. Zhang, Talanta 73 (2007) 366–371.
[17] L.L. Zhang, X.W. Zheng, Anal. Chim. Acta 570 (2006) 207–213.
[18] Z.Y. Zhong, M.X. Li, D.B. Xiang, N. Dai, Y. Qing, D. Wang, D.P. Tang, Biosens. Bioelectron. 24 (2009) 2246–2249.
[19] J. Zhao, Y.Y. Zhang, H.T. Li, Y.Q. Wen, X.Y. Fan, F.B. Lin, L. Tan, S.Z. Yao, Biosens. Bioelectron. 26 (2011) 2297–2303.
[20] L. Kokko, T. Kokko, T. Lövgren, T. Soukka, Anal. Chim. Acta 606 (2008) 72–79.
[21] S. Zanarini, E. Rampazzo, L. Della Ciana, M. Marcaccio, E. Marzocchi, M. Montalti, F. Paolucci, L. Prodi, J. Am. Chem. Soc. 131 (2009) 2260–2267.
[22] X.Y. Yang, Y.S. Guo, S. Bi, S.S. Zhang, Biosens. Bioelectron. 24 (2009) 2707–2711.
[23] J. Wang, G.D. Liu, M.H. Engelhard, Y.H. Lin, Anal. Chem. 78 (2006) 6974–6979.
[24] X.M. Chen, Z.J. Lin, Z.M. Cai, X. Chen, M. Oyama, X.R. Wang, J. Nanosci. Nanotechnol. 9 (2009) 2413–2420.
[25] G.H. Zuo, Q. Huang, G.H. Wei, R.H. Zhou, H.P. Fang, ACS Nano 4 (2010) 7508–7514.
[26] T. Fonong, G.A. Rechnitz, Anal. Chem. 56 (1984) 2586–2590.
[27] X. Lu, Q.Z. Song, G.L. Ma, Med. Lab. Sci. Clinics 19 (2008) 58–59.